

## Subaru Suprime-Cam Weak Lensing Survey Over 33 deg<sup>2</sup> — Suprime33

Satoshi Miyazaki

*Subaru Telescope/NAOJ, 650 N Aohoku Pl. Hilo HI 96720 USA*

Takashi Hamana

*Institut d'Astrophysique de Paris, 98bis Boulevard Arago, 75014 Paris, France/ National Astronomical Observatory of Japan, Mitaka, Tokyo 181-8588, Japan*

Alexandre Refregier

*Service d'Astrophysique CEA Saclay, Bat. 709 F-91191 Gif sur Yvette, France*

Richard Ellis

*California Institute of Technology, 105-24 Astronomy, Caltech, Pasadena CA 91125 USA*

**Abstract.** We have demonstrated that newly developed Suprime-Cam on the 8-m Subaru telescope is capable of blind searches of mass concentration via weak lensing. We then propose to extend the survey up to 33 square degrees where archival X-ray data is available (*Suprime33* Survey). The survey status and the performance of Suprime-Cam in the weak lensing survey are shown.

### 1. Introduction

Suprime33 is a weak lensing survey which exploits the unique capabilities of Suprime-Cam (Miyazaki et al. 2002b). Its purpose is to construct, for the first time, a *mass selected* cluster catalog. The primary science goal of Suprime33 is to test the structure formation paradigm with a well-defined mass-limited cluster catalog. One of the most important and unambiguous tests of this paradigm concerns the abundance of halos and its evolution with redshift. These have been extensively studied using *N*-body simulations (e.g. Jenkins et al. 2001), and are regarded as well-established theoretically. Therefore, the comparison between the theoretical prediction and our weak lensing measurement is one of the simplest and the most direct methods to test the paradigm. This test has not yet been achieved because it requires large observational resources. As an example, Figure 1 shows the predicted redshift distribution of clusters assuming a  $\Lambda$ CDM model. If our mass-selected clusters show a completely different distribution with redshift, then it would be a serious challenge to the CDM paradigm. Note that the number of clusters in our sample is sufficient to discriminate  $\Lambda$ CDM

and  $\Lambda$ CDM if we have about 100 cluster samples, which we set as the minimum goal of the survey.

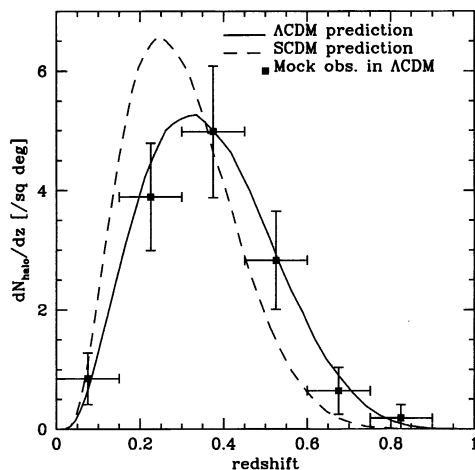


Figure 1. Redshift distribution of clusters detectable through our Suprime-Cam weak lensing survey. Points with errors bars show the expected accuracy of the proposed survey over  $33 \text{ deg}^2$  assuming a  $\Lambda$ CDM model ( $\Omega_m = 0.3$ ,  $\Omega_\Lambda = 0.7$ ,  $\sigma_8 = 0.9$ ). The dashed line shows the prediction for a SCDM model ( $\Omega_m = 1$ ,  $\Omega_\Lambda = 0$ ,  $\sigma_8 = 0.6$ ).

Using GTO data obtained by Suprime-Cam over a contiguous  $2 \text{ deg}^2$  field ( $3 \times 3$  Suprime-Cam pointings), we have demonstrated the first reliable detection of  $\simeq 5$  mass concentrations with  $S/N > 5$  (Figure 2, Miyazaki et al. 2002a). In order to quantify the reliability of the detection, we examine the probability distribution function (PDF) of peaks on the  $S/N$  map. The peaks are identified by pixels having a higher or lower value of  $S/N$  than all eight surrounding pixels, as suggested by Jain & van Waerbeke (2000). The PDF of the peak heights is shown as thick histograms in Figure 3. The thin histogram shows a noise PDF which is the average of 100 randomizations, and the error bars show the rms among them. Excess counts over the noise PDF are apparent. Figure 3 shows that approximately 30 % of peaks are spurious if one sets the threshold of the detection at  $S/N = 3$  on the  $\theta_G = 1'$  map. If one increases the threshold up to 5, the spurious peaks created by the noise are negligible in this  $2 \text{ deg}^2$  GTO field. Assuming the number density of  $\sim 3$  per  $\text{deg}^2$  ( $S/N > 5$ ) obtained here, we must observe  $\sim 30 - 40 \text{ deg}^2$  to secure  $\sim 100$  samples. This is why we are proposing to survey over  $33 \text{ deg}^2$ .

Hamana et al. (2004) examined the efficiency of the weak lensing survey in detail using numerical simulation and showed that the rate of spurious detection due to the noise can be as high as 10 % even if we set the threshold at  $S/N = 5$ . The rate seems higher than what is expected from the GTO results (Figure 3), but the GTO  $2 \text{ deg}^2$  field is too narrow to compare with the results from large scale simulations ( $106 \text{ deg}^2$ ). When we select the secure candidate clusters for spectroscopic follow-up, we use cross correlation of the weak lensing mass with density enhancement of relatively bright galaxies to find the spurious detection minimum. Super-position of multiple clusters, which are located at different

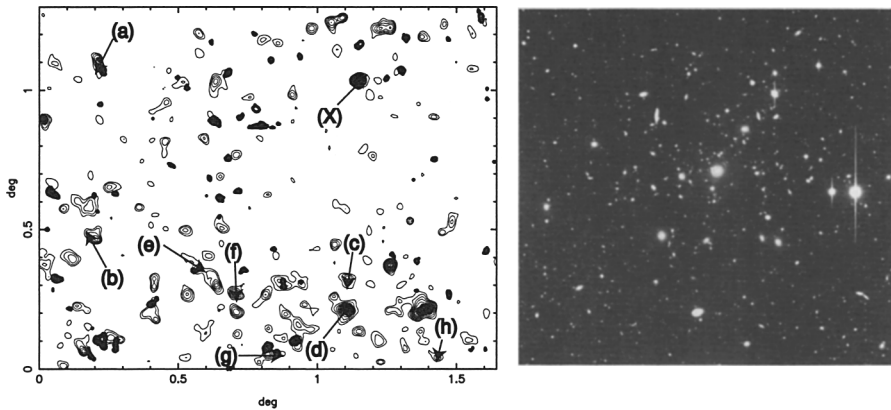


Figure 2. **(Left)** Demonstrating Suprime-Cam’s ability for locating mass concentrations (or halos) from weak lensing data in the 2 deg<sup>2</sup> GTO field (Miyazaki et al 2002a). Thick contours indicate mass over-densities where the lensing (convergence) signal/noise exceeds 3. Thin contours show the surface density of visible ( $20 < R < 23$ ) galaxies. Regions marked (a-h) represent known clusters which clearly constitute only a fraction of the massive structures detected in this field. **(Right)** Optical counterpart of halo X (see left panel) identified as a new cluster at  $z = 0.41$  with subsequent FOCAS spectroscopy. This cluster is not listed in the NASA/IPAC NED catalog.

distances along the line of sight, can produce significant lensing signal even though the mass of each cluster is small. Although numerical simulation showed that such chance projection rate is small, we will be able to discriminate these objects from our cluster samples using the spectroscopic data.

## 2. Suprime33 Survey

In the Apr-Sep semester of 2003, our Suprime33 survey was awarded five nights as a Subaru intensive program. We chose the survey area where ROSAT/PSPC’s deep pointings X-ray data ( $T_{exp} > 25$  ksec) are available. In May and September 2003, we have obtained images over 12.5 deg<sup>2</sup> whose seeing is better than 0.8 arcsec and are thus suited for weak lensing analysis (8.5 deg<sup>2</sup> in May and 4 deg<sup>2</sup> in September). The median seeing is about 0.7 arcsec (See Figure 4). We also examined Suprime-Cam public data to select fields which satisfy our survey criteria (especially the depth of the X-ray data available in the field). We found 4.5 deg<sup>2</sup> of suitable area in the archive. We have performed the weak lensing analysis of all the data except that taken during the September run (Miyazaki et al. in preparation).

In the preliminary results for the 13 deg<sup>2</sup> data, we have identified 20 peaks, whose weak lensing signal is significant ( $S/N > 5$ ), and which match the galaxy density enhancement of  $3\sigma$  over the average within a radius of 2 arcmin. We refer to these objects as secure candidates of clusters of galaxies. Note that none of them is listed in the NASA Extra-galactic Database (NED), except one GHO cluster (GHO1601+4253). If we lower the threshold of the shear signal

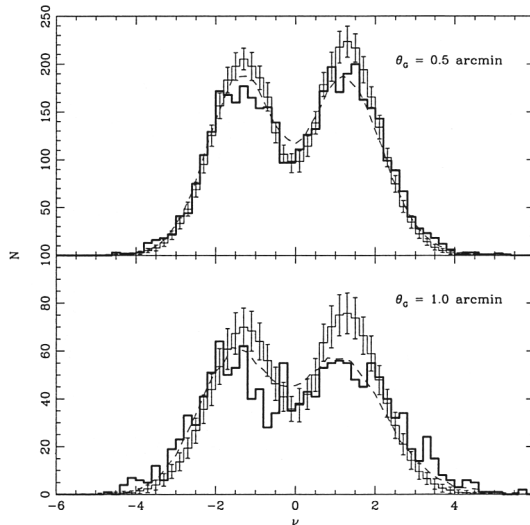


Figure 3. Peak distribution function in a  $\kappa$  map with smoothing scale  $\theta_G = 0'.5$  (top) and  $1'$  (bottom). Thick solid histograms show the results obtained from the observed catalog and thin solid histograms associated with error bars are averaged results of 100 random realizations of galaxy orientation in the catalog. The errors are the rms of the randomization. The excess count over the noise becomes more apparent as the gaussian smoothing scale ( $\theta_G$ ) on the S/N map increases.

to  $S/N > 4$ , the number of mass concentrations exceeds 60 but approximately 20% of the peaks may be spurious according to the simulation by Hamana et al. (2004).

The X-ray detection flux limit is lower than  $f_{[0.5-2\text{keV}]} = 9 \times 10^{-14} \text{ erg cm}^{-2} \text{ s}^{-1}$  for all of the fields, which corresponds to  $L_x \sim 4 \times 10^{43} \text{ erg s}^{-1}$  for clusters at  $z = 0.5$ . We do not use X-ray data to select the follow-up candidates since it may cause a bias toward X-ray luminous objects. In fact, some of the cluster candidates are obviously missing from earlier X-ray surveys. We are proposing to carry out a multi-slit spectroscopic follow-up of the secure candidates in order to obtain their redshift and their velocity dispersion. As we have already demonstrated by the GTO  $2 \text{ deg}^2$  survey followed by FOCAS spectroscopic observations, significant mass concentrations ( $S/N > 5$ ) associated with high galaxy density are likely to be actual clusters.

### 3. Suprime-Cam Image Quality

The primary source of the noise on the mass map is the intrinsic variance of galaxy ellipticities,  $\sigma_\epsilon$  ( $\sim 0.4$ ). The noise,  $\sigma_{noise}$  is expressed as

$$\sigma_{noise} = \frac{\sigma_\epsilon}{2\sqrt{\pi n_g}} \theta_G^{-1} \quad (1)$$

$$= 0.02(\sigma_\epsilon/0.4)(n_g/40)^{-1/2} \theta_G^{-1}, \quad (2)$$

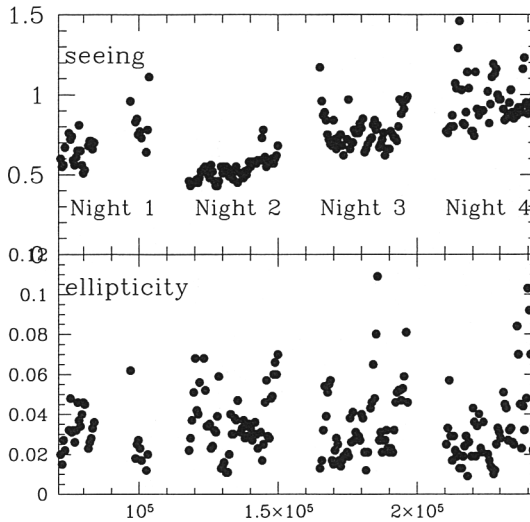


Figure 4. The seeing (in arcsec) and rms of raw ellipticities averaged over moderately bright stars on the Suprime-Cam field of view ( $34' \times 27'$ ). Each point shows the result of one 7.5 minute exposure. The horizontal axis shows the progress of time in seconds, but the time between nights is arbitrarily deducted for presentation.

where  $n_g$  and  $\theta_G$  are the galaxy surface density in  $\text{arcmin}^{-2}$  and the gaussian smoothing scale of the mass map, respectively. The noise can be effectively reduced by increasing the number of faint galaxies. This is why we need a large aperture telescope to obtain deeper images. In the case of Suprime-Cam, an exposure of 30 minutes in  $R$ -band gives  $40 \text{ galaxies arcmin}^{-2}$ . The smoothing scale is chosen so that the number of clusters detected is maximized. According to the simulation by Hamana et al. (2003),  $\theta_G = 1 \text{ arcmin}$  is a reasonable choice. Then, we have  $\sigma_{noise} = 2\%$ . In the meantime, a typical massive cluster ( $M \sim 10^{14} M_\odot$ ) at the redshift of 0.3-0.7 produced the convergence signal of 0.1, resulting in the detection of  $S/N = 0.1/0.02 = 5$ .

In the real world, image degradation due to an imperfect measurement system can be additional noise sources. This should be small compared with the  $\sigma_{noise}$  described above. The degradation is usually characterized by ellipticities of stars, which is the simplest representation of the PSF anisotropy. The bottom panel of Figure 4 shows the rms value of ellipticities obtained during the four consecutive nights of the May observing run. Seeing in arcsec (FWHM) is also shown in the upper panel for reference. The ellipticities are the averaged value of all the stars over the field of view ( $\sim 1000$  stars in  $34' \times 27'$ ). Note that the ellipticities are mostly  $2\% \sim 4\%$ , and that there are few cameras besides Suprime-cam that can achieve such low stellar ellipticities under good seeing ( $< \sim 0.8 \text{ arcsec}$ ).

Since the rms of ellipticities is comparable to the  $\sigma_\epsilon$ , it is already feasible to use the raw ellipticities to search for mass concentration. However, some PSF correction procedures should be employed to reduce the noise further; i.e. to suppress the spurious detection of peaks. We model the ellipticities of stars by

fitting to the fifth order bi-polynomial function of field position over the entire field of view. As a result of this simple correction, the rms value is reduced to 1.2% – 1.5%, which is small enough for the weak lensing cluster survey. In other words, the weak lensing signal induced by a cluster of galaxies is large enough to make this level of noise acceptable practically. Signals induced by large scale structure (called cosmic shear), however, are more subtle at about 1%. In this case, extreme care should be taken in dealing with the correction of PSF anisotropy because the degree of correction is comparable to the signal itself. We are now working on detailed characterization of the PSF anisotropy of Suprime-Cam to resolve this issue.

## References

- Hamana, T., et al. 2004, MNRAS, 350, 893  
Jain, B., & van Waerbeke, L. 2000, ApJ, 530, L1  
Jenkins, A., et al. 2001, MNRAS, 321, 372  
Miyazaki, S., et al. 2002a, ApJ, 580, L97  
Miyazaki, S., et al. 2002b, PASJ, 54, 833